



## Analysis of OCR and GFR Coordination on the 20 kV Cubicle at Mosad Office Tower Samarinda

Masing<sup>1</sup>, Syamsul Rizal Fadhil<sup>2</sup>, Onglan Nainggolan<sup>3</sup>, Rizky Aprylianto Susilo<sup>4</sup>, Wahyu Setiawan<sup>5</sup>

<sup>1,2,3,4,5</sup> Department of Electrical Engineering, Samarinda State Polytechnic

**ABSTRACT:** The distribution system is a component of the electric power system responsible for delivering electricity from the transmission network to consumers. This system generally utilizes medium voltage levels, which are more susceptible to faults compared to transmission systems. To mitigate disturbances in the distribution network, protection equipment is employed. Commonly used protection devices include the Overcurrent Relay (OCR) and the Ground Fault Relay (GFR). Coordination between the OCR and GFR is essential to ensure the protection system functions optimally, possesses adequate selectivity and sensitivity, and maintains the continuity of electricity supply. This paper discusses the coordination settings of the overcurrent and ground fault relays. Simulations were conducted using ETAP 19.0.1 software based on field data. Calculation results on the feeder indicate an OCR grading time of 0.489 seconds, whereas the field data shows 0.4 seconds. For the GFR, the grading time on the feeder is 0.297 seconds, compared to 0.4 seconds from the field data. These values indicate that the protection coordination within this system can be considered ideal.

**KEYWORDS:** Ground fault relay, Overcurrent relay, Protection coordination, ETAP 19.0.1

### I. INTRODUCTION

The electrical energy distribution system is a critical component of the power system, responsible for delivering electricity from generation sources to consumers. As the population grows and the number of electricity users increases annually, the risk of faults occurring within the distribution system also rises [1].

With the increasing demand for electricity, power systems have become increasingly complex, requiring effective control to ensure efficient energy distribution. The distribution system plays a pivotal role in transmitting electricity from substations to consumers via Medium Voltage Overhead Lines (SUTM) and Medium Voltage Underground Cables (SKTM). Supporting equipment, such as medium voltage cubicles, is required to function as connectors, breakers, dividers, and controllers of the power flow. Consequently, distribution networks must be meticulously designed and supported by adequate investment and high-quality equipment to ensure future reliability [2].

One common issue in electrical distribution networks is short-circuit faults, occurring either between phases or between a phase and the ground. These faults can be caused by insulation failure, technical errors, pollution, or environmental conditions surrounding the network. To address these issues, a protection system comprising Current Transformers (CT), Potential Transformers (PT), circuit breakers, connecting cables, and protection relays working in an integrated manner is employed. Among these components, the protection relay plays a vital role in detecting and responding to system faults [3].

The most frequent faults in distribution systems are short circuits, including three-phase, phase-to-phase, and phase-to-ground faults. To detect these, Overcurrent Relays (OCR) and Ground Fault Relays (GFR) are utilized. The primary protection is designed to operate first at the location nearest to the fault, while backup protection will operate should the primary protection fail [4].

Protection system coordination aims to determine the precise operating time settings during a fault event. This is achieved by adjusting protection values appropriately so that each device functions effectively. Proper coordination is necessary to isolate the fault area and minimize the resulting impact [1].

### II. RESEARCH METHODOLOGY

#### A. Research Location and Duration

This research was conducted at the Mosad Office Tower Samarinda, located at Jalan Cipto Mangun Kusumo, Sungai Keledang, Samarinda Seberang District, Samarinda City, East Kalimantan. The research commenced in January and continued until the study was declared complete.

**B. Data Types and Sources**

This research employs a qualitative method utilizing a direct observation approach. The study commences with field data collection, which is subsequently analyzed to address the problem formulation. The data sources in this study consist of both primary and secondary data. Primary data was obtained through interviews and discussions with relevant on-site personnel as well as academic supervisors. Meanwhile, secondary data was derived from documents, reports, literature, scientific journals, books, websites, and manufacturer information supporting the thesis compilation.

**C. Research Flowchart**

The research flowchart serves as a visual representation illustrating the systematic stages of the research process. This diagram depicts the workflow, originating from problem identification, objective definition, and data collection and analysis, to the formulation of conclusions and the reporting of results. The utilization of a flowchart ensures the research process remains structured and easily comprehensible.

1) Research Concept Flowchart

The research concept flowchart is a systematic representation of the researcher's thought process, linking key components within the study, ranging from the scope and problem limitations to the final objective. This entire process is structured in the form of a diagram to clarify the direction and stages of the research, as shown in Figure 1 below.

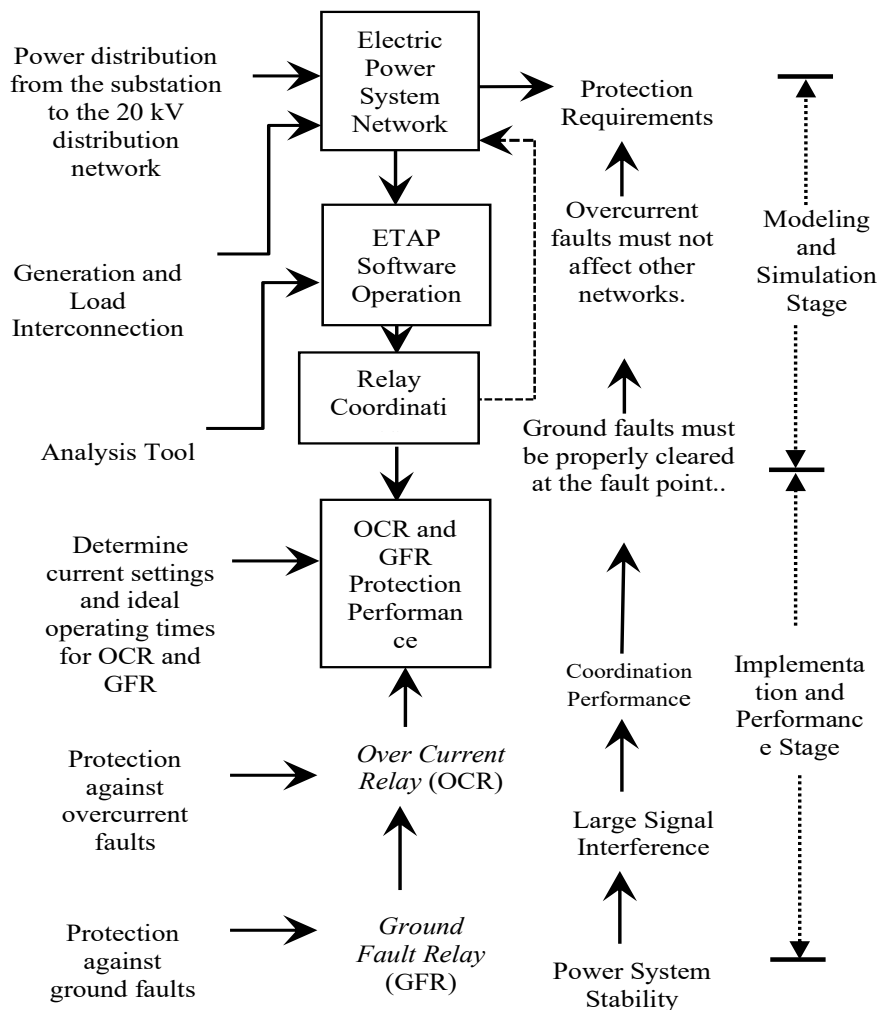


Figure 1. Research Concept Flowchart

2) Operational Research Flowchart

The research commences with a preliminary study, which encompasses theoretical data collection through a literature review and an assessment of field conditions via a case study. This stage serves as the foundation for comprehending the operating principles of relays and the protection coordination concepts that will be analyzed subsequently.

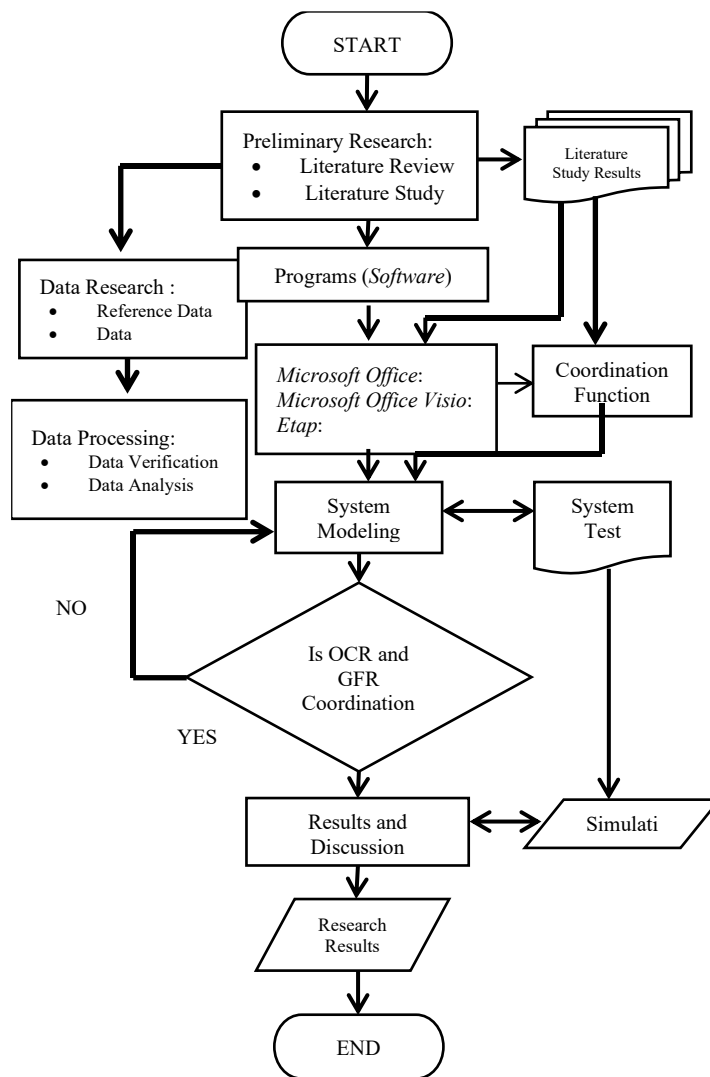


Figure 2. Operational Research Flowchart

III. RESULT AND DISCUSSION

A. Harapan Baru Substation Source Impedance

The short-circuit capacity on the primary side bus of the transformer (150 kV) at Karang Joang Substation was recorded at 133,307.3 MVA. Based on this value, calculations were performed to determine the source impedance (Xs) on the primary side, yielding a value of 0.17Ω. This value represents the total system impedance opposing fault currents on the high-voltage side. Subsequently, this impedance was referred to the transformer's secondary side—specifically the 20 kV bus—taking into account the transformation ratio and equipment characteristics, resulting in an impedance value of 0.003Ω. This significantly lower impedance value on the secondary side indicates that the prospective fault current on the lower voltage side will be much higher. Therefore, this must be addressed through precise protection system settings to ensure the reliability and safety of distribution network operations.



**B. Transformer Impedance**

The transformer installed at the Mosad Office Tower has an impedance of 4.5%. Based on this data, the positive and negative sequence reactance values ( $X_{t1} = X_{t2}$ ) of the transformer are 22.5  $\Omega$ . This transformer is utilized to supply the feeder and features a YNyn0+d connection configuration, which includes a delta winding. Due to the presence of this delta winding, the zero-sequence reactance value ( $X_{t0}$ ) is 225  $\Omega$ .

**C. Distribution Network Impedance**

Based on the data obtained, the feeder utilizes an AAAC (All Aluminum Alloy Conductor) type with a cross-sectional area of 150 mm<sup>2</sup>. The length of the HRB 6 feeder is 4.8 km. Assuming that faults occur at specific points along the feeder—specifically at distances of 0%, 20%, 40%, 60%, 80%, and 100% of the total feeder length—the impedance values for the HRB 6 feeder can be calculated based on these fault locations, as presented in Table 1 and Table 2.

**Table 1. Positive and Negative Sequence Feeder Impedance**

% Feeder Length	$Z_1 = Z_2$ ( $\Omega/\text{km}$ )	Total Length
0	$0 \times 4,8 \times (0,2162 + j 0,3305)$	$0 \Omega$
25	$0,25 \times 4,8 \times (0,2162 + j 0,3305)$	$0,26 + j 0,396 \Omega$
50	$0,50 \times 4,8 \times (0,2162 + j 0,3305)$	$0,518 + j 0,793 \Omega$
75	$0,75 \times 4,8 \times (0,2162 + j 0,3305)$	$0,778 + j 1,189 \Omega$
100	$1 \times 4,8 \times (0,2162 + j 0,3305)$	$1,037 + j 1,586 \Omega$

**Table 2. Zero-Sequence Feeder Impedance**

% Feeder Length	$Z_0$ ( $\Omega/\text{km}$ )	Total Length
0	$0 \times 4,8 \times (0,3631 + j 1,6180)$	$0 \Omega$
25	$0,25 \times 4,8 \times (0,3631 + j 1,6180)$	$0,435 + j 1,941 \Omega$
50	$0,50 \times 4,8 \times (0,3631 + j 1,6180)$	$0,871 + j 3,883 \Omega$
75	$0,75 \times 4,8 \times (0,3631 + j 1,6180)$	$1,307 + j 5,854 \Omega$
100	$1 \times 4,8 \times (0,3631 + j 1,6180)$	$1,742 + j 7,766 \Omega$

**D. Equivalent Feeder Impedance**

The equivalent impedances utilized in this analysis encompass the positive-sequence equivalent impedance ( $Z_{1eq}$ ), negative-sequence equivalent impedance ( $Z_{2eq}$ ), and zero-sequence equivalent impedance ( $Z_{0eq}$ ). Calculations for each type of equivalent impedance were conducted at distances of 0%, 20%, 40%, 60%, 80%, and 100% of the feeder length. The results of these calculations are presented in Table 3 and Table 4 below.



Table 3. HRB6 Feeder Equivalent Impedance ( $Z_{1ek}$  &  $Z_{2ek}$ )

Network Length (%)	Length (km)	$Z_{1ek} = Z_{2ek}$	Total
0%	0	$j0,003 + 22,5 + 0$	$22,5 + j 0,003$
25%	1,2	$j0,003 + 22,5 + (0,26 + j 0,396)$	$22,76 + j 0,399$
50%	2,4	$j0,003 + 22,5 + (0,518 + j 0,793)$	$23,018 + j 0,796$
75%	3,6	$j0,003 + 22,5 + (0,778 + j 1,189)$	$23,278 + j 1,192$
100%	4,8	$j0,003 + 22,5 + (1,037 + j 1,586)$	$23,537 + j 1,589$

Table 4. HRB 6 Feeder Zero-Sequence Equivalent Impedance

Network Length (%)	Length (km)	$Z_{0ek}$	Total
0%	0	$j225 + (3 \times 0) + 0$	$0 + j 255$
25%	1,2	$j225 + (3 \times 0) + (0,435 + j 1,941)$	$0,435 + j 226,941$
50%	2,4	$j225 + (3 \times 0) + (0,871 + j 3,883)$	$0,871 + j 228,883$
75%	3,6	$j225 + (3 \times 0) + (1,307 + j 5,854)$	$1,307 + j 230,854$
100%	4,8	$j225 + (3 \times 0) + (1,742 + j 7,766)$	$1,742 + j 232,766$

**E. Short-Circuit Current Calculation**

Short-circuit fault currents in electrical distribution systems can be calculated by applying Ohm's law; however, the equivalent impedance values utilized in these calculations vary depending on the specific type of fault encountered. typically, the fault types analyzed include three-phase short-circuit faults, which generally yield the highest fault currents, and single-phase-to-ground faults, which are frequently encountered in distribution systems.

For the HRB 6 feeder, short-circuit current calculations based on these two fault types were conducted by accounting for the impedance of each system component. A summary of these calculation results is presented in Table 5 to serve as a reference for determining precise and reliable protection settings.

Table 5. Calculation Results of Short-Circuit Fault Currents for HRB 6 Feeder

Short-Circuit Fault Type	Calculation Results	ETAP Simulation Results
1 Phase	0,143713 kA	0,142 kA
3 Phase	0,51320 kA	0,513 kA



**F. OCR and GFR Setting Calculations**

On the HRB 6 feeder at Harapan Baru Substation, a current transformer (CT) with a ratio of 300:5 A is installed, serving as the reference for calculating the pick-up level and Time Multiple Setting (TMS). Based on the calculation results presented in Table 10 and Table 11, the HRB 6 feeder—characterized by a total load of 800 kW and a line length of 4.8 km—requires an OCR current setting of 22 A with a TMS of 0.040 seconds on the feeder side. Conversely, the incoming side is configured with a current setting of 5.5 A and a TMS of 0.044 seconds. Regarding the GFR settings for the HRB 6 feeder, the incoming side is adjusted to a current of 0.21 A with a TMS of 0.2 seconds. Meanwhile, the feeder side utilizes the same current setting of 0.21 A but with a lower TMS of 0.1 seconds. This configuration is intended to ensure effective and selective protection coordination against potential faults within the distribution network.

**Table 6. OCR And GFR Setting Results for HRB 6 Feeder**

Relay Type	Relay Location	Iset (A)	TMS	Time (seconds)	Grading Time
Overcurrent Relay (OCR)	Incoming	5,5	0,044	0,631	0,489
	Feeder	22	0,040	0,142	
Ground Fault Relay (GFR)	Incoming	0,21	0,2	0,594	0,297
	Feeder	0,21	0,1	0,297	

**G. OCR and GFR Coordination**

Based on the simulation results presented in the figure above, it is observed that the GFR—being the relay closest to the fault location—operates first when a fault occurs. Consequently, the Circuit Breaker (CB) associated with the GFR will clear the fault current. Meanwhile, the OCR serves as backup protection and will operate should the GFR fail to function. The operating times for both relays are displayed in the coordination curves in Figure 3 and Figure 4 as follows.

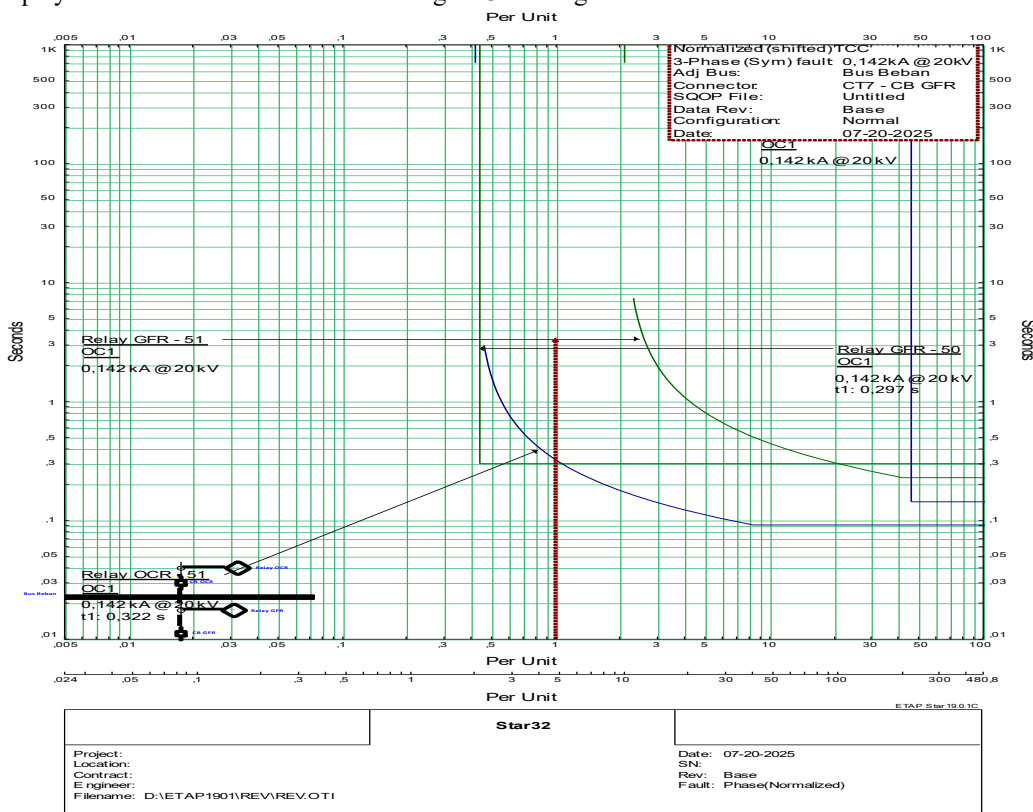


**Figure 3. Relay time selectivity curve results on the feeder side with grid lines**

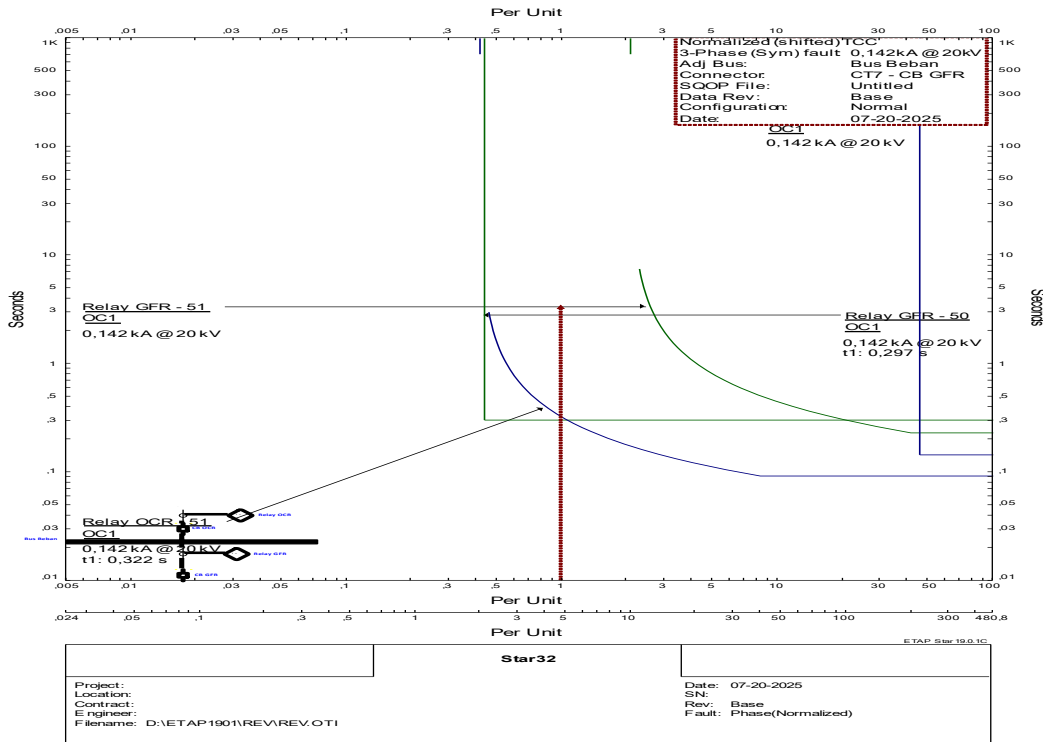


Figure 4. Relay time selectivity curve results on the feeder side

In the coordination curve obtained from the simulation on the feeder side, it is observed that the GFR—acting as the relay closest to the fault point—operates first with an operating time of 0.297 seconds. Meanwhile, the OCR functions as backup protection and will operate at 0.631 seconds should the GFR fail to operate.

IV. CONCLUSION

Manual calculations yielded a three-phase short-circuit current of 0.51320 kA, whereas the ETAP 19.0.1 simulation indicated 0.513 kA. For the single-phase-to-ground fault, values of 0.143713 kA and 0.142 kA were obtained from manual calculations and the simulation, respectively. This slight discrepancy is attributed to variations in system assumptions and parameters; however, both remain consistent in representing the fault current magnitude. Calculation results indicate an OCR operating time of 0.631 seconds and a GFR operating time of 0.594 seconds. The OCR prioritizes the response to phase faults, while the GFR addresses ground faults. This distinction ensures selective and reliable protection coordination. Furthermore, regarding the relay operating time settings on the feeder side, the OCR operating time was determined to be 0.142 seconds, and the GFR operating time was 0.297 seconds. This demonstrates that the feeder relay is designed to respond rapidly to faults, whether phase or ground-related.

REFERENCES

1. R. Adzin, "Coordination Analysis of Overcurrent Relay (OCR) and Ground Fault Relay (GFR) in 20 kV Medium Voltage Power Distribution Systems (Case Study at PT. PLN (Persero) ULP Sidareja)," *Universitas Peradaban Library*, 2022. Accessed: Nov. 01, 2024.
2. A. El, Joko Joko, T. Rijanto, and T. Wrahatnolo, "Testing of Overcurrent and Ground Fault Relay Coordination as Protection and Safety Measures in 20 kV Cubicles in Electric Power Distribution Systems," *Scientica: Scientific Journal*,
3. S. Thaha, A. W. Indrawan, and Y. J. Pongkiding, "Analysis of the Protection Coordination System for Overcurrent Relay (OCR) and Ground Fault Relay (GFR) on the 20 kV Transformer Bay at Sanga-Sanga Substation, East Kalimantan,"
4. R. Andriyan, Nasrulloh, and R. Murdiantoro, "Analysis of Coordination of Overcurrent Relay (OCR) and Ground Fault Relay (GFR) on the 20 kV Distribution System: A Case Study at PT. PLN (Persero) ULP Sidareja,



5. J. M. Siburian, T. Siahaan, and J. Sinaga, "Analysis of 20 kV Distribution Network Performance Improvement Using Thermovision Method on the Network of PT. PLN (Persero) ULP Medan Baru," *Uda Energy Technology Journal: Journal of Electrical Engineering*, vol. 9, no. 1, pp. 8–19, 2020. Accessed: Nov. 18, 2024. [Online].
6. H. D. Paminto and A. Kiswantono, "Simulation Design of Overcurrent Relay System on 20 kV Distribution Networks," *Aisyah Journal of Informatics and Electrical Engineering (AJIEE)*, vol. 3, no. 1, pp. 45–49, Feb. 2021.
7. M. Y. Imanuddin and F. Achmad, "Design of Power Distribution Protection System for the Kyo Apartment Project at PT. Alkonusa Teknik Interkon," *Journal of Education and Counseling (JPDK)*, vol. 5, no. 1, pp. 1633–1639, 2023.
8. W. Sarimun N., *Technical Services Pocket Book*, 2nd ed. Depok, Indonesia: Garamond, 2011.

---

*Cite this Article: Masing, Fadhil, S.R., Nainggolan, O., Susilo, R.A., Setiawan, W. (2025). Analysis of OCR and GFR Coordination on the 20 kV Cubicle at Mosad Office Tower Samarinda. International Journal of Current Science Research and Review, 8(11), pp. 5788-5795. DOI: <https://doi.org/10.47191/ijcsrr/V8-i11-35>*